

## Origin of Resistive-Switching Behaviors of Chemical Solution

### Deposition-derived BiFeO<sub>3</sub> thin-film Memristors

Feng Yang,<sup>1\*</sup> Fen Liu,<sup>2</sup> Fengqi Ji,<sup>1</sup> Yanlin Lin,<sup>1</sup> Minghua Tang<sup>3</sup>

1. School of Materials Science and Engineering, University of Jinan, Jinan 250022, People's Republic of China.

2. Shandong Provincial Key Laboratory of Preparation and Measurement of Building Materials, University of Jinan, Jinan 250022, People's Republic of China.

3. Hunan Provincial National Defense Key Laboratory of Key Film Materials & Application for Equipments, Xiangtan 411105, People's Republic of China.

\*E-mail: mse\_yangf@ujn.edu.cn

**Keywords:** ferroelectric thin film, ferroresistive switching, resistive switching, BiFeO<sub>3</sub>, memristor

#### Supporting Information

##### 1. Polarization–voltage hysteresis loops

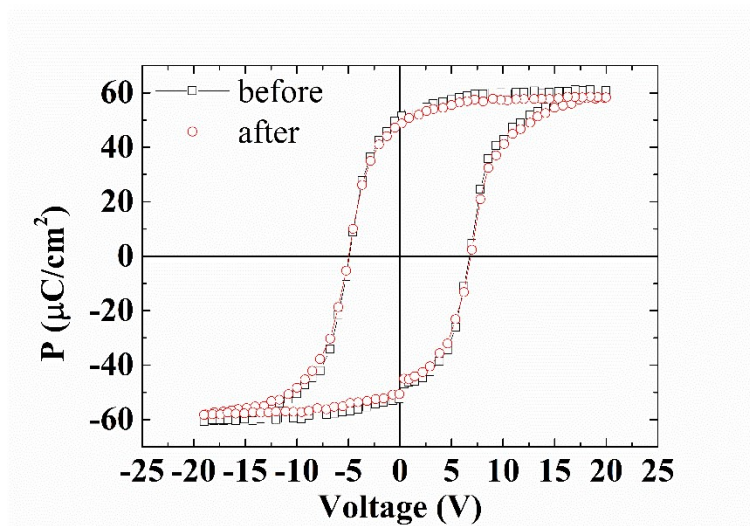


Fig. S1. The polarization–voltage hysteresis loops of the BFO memristor before and after several RS cycles under high DC voltages of  $\pm 20 \text{ V}$ .

##### 2. Fatigue behavior

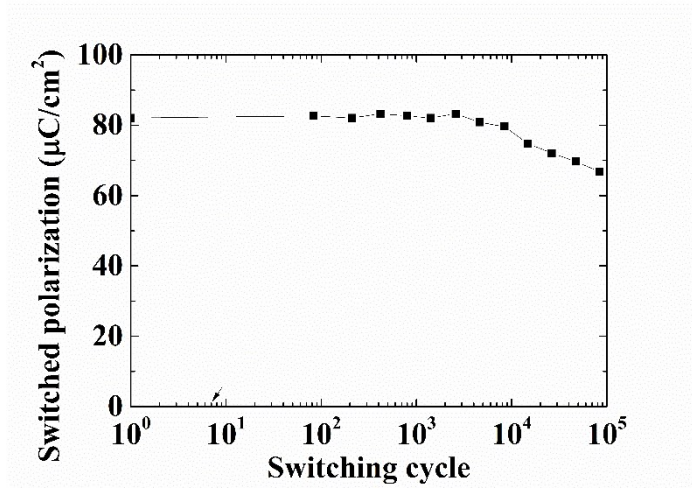


Fig. S2. Fatigue behavior of BiFeO<sub>3</sub> films.

### 3. Physical mechanism of the RS

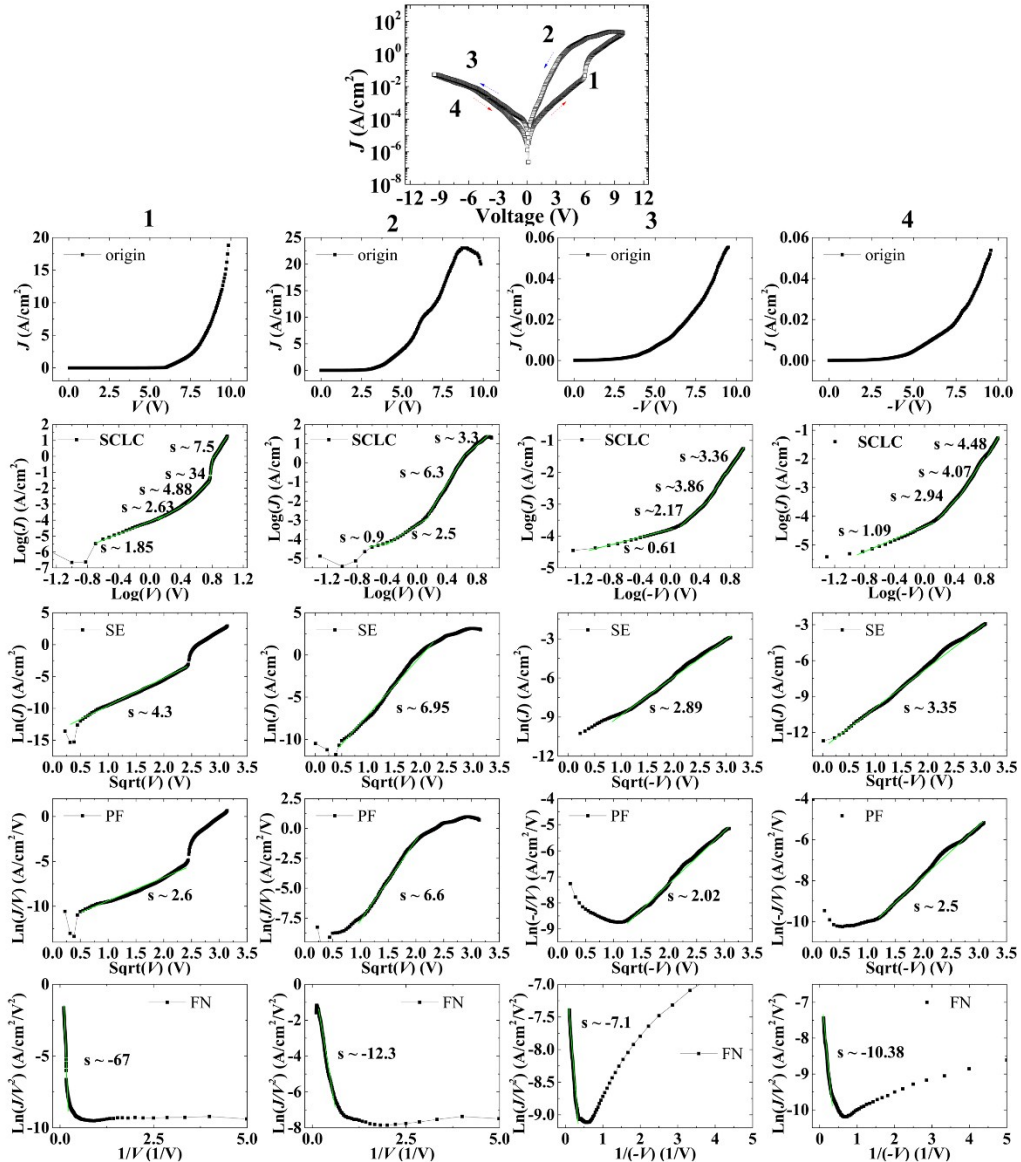


Fig. S3 Plots of the  $I$ - $V$  curves in Fig. 1(d) on different scales to reveal their conduction mechanisms: space-charge-limited conduction (SCLC), Schottky emission (SE), Poole–Frenkel emission (PF), and Fowler–Nordheim (FN) tunneling.

To further investigate the physical mechanism related to the RS of the Pt/BFO/LSMO heterostructure, analysis on the internal conductive-transport properties is necessary. The most possible conductive mechanisms include SCLC, SE, FN tunneling, and PF.<sup>[1-3]</sup> FN tunneling and Schottky conduction are electrode/bulk interface-dominated mechanisms, whereas SCLC and PF are bulk-limited conduction mechanisms. If leakage was controlled by PF emission, which originated from the field-assisted thermal ionization of trapped carriers into the conduction band of the semiconductors, then the leakage current density would be expressed as follows<sup>[4]</sup>:

$$J_{PF} = cE \exp\left[e\left(\sqrt{eE/\pi\epsilon_0\epsilon_{ro}} - E_t\right)/kT\right],$$

where  $c$  is a constant,  $e$  is the electronic charge,  $k$  is the Boltzmann constant,  $T$  is the temperature in Kelvin,  $\epsilon_0$  is the permittivity of free space,  $\epsilon_{ro}$  is the optical dielectric constant of the film,  $E_t$  is the trap ionization energy,  $E$  is the applied electric field, and the relationship with the voltage satisfies  $E = V/d$ . The PF emission produces a linear relation between  $\ln J/V$  and  $V^{1/2}$ . The interface-limited FN tunneling, which may substantially contribute to the leakage current at high applied electric fields, can be described by the following relationship<sup>[5]</sup>:

$$J_{FN} = BE^2 \exp(-C\varphi_i^{3/2}/E),$$

where  $B$  and  $C$  are constants, and  $\varphi_i$  is the potential barrier height. If the leakage current was dominated by FN tunneling, a linear relation between  $\ln J/E^2$  and  $1/E$  would be observed.

However, no linear relations were observed in the PF emission model with  $\ln J/E$  versus  $E^{1/2}$  and the FN tunneling model with  $\ln J/E^2$  versus  $1/E$  (Fig. S1). Overall, no linear relationship existed, but the linear part locally appeared. In particular, the FN mechanism exhibited a negative-slope linear part in the larger voltage part, consistent with the quantum-tunneling mechanism through a very thin insulating layer at the BFO/LSMO interface. An imperfect linear relationship also existed in the PF simulation, so the PF mechanism cannot be completely ruled out.

The interface-limited SE, which is based on the Schottky barrier at the interface of the metal electrode and the dielectric, can be described as follows<sup>[5]</sup>:

$$J_{SE} = AT^2 \exp(-\varphi_b/kT) \exp\left[e\sqrt{eE/4\pi\epsilon_0\epsilon_{ro}}/kT\right],$$

where  $A$  is the Richardson constant and  $\varphi_b$  is the Schottky barrier height. If the interface leakage current was indeed controlled by the SE, then the plot of  $\ln J-V^{1/2}$  would be a straight line. As shown in the image, a very good linear relationship existed.

According to Lampert's theory regarding SCLC in insulators,<sup>[6]</sup> each leakage current behavior can be divided into several different regions dominated by  $J_{SCLC} \propto V^\alpha$ , where  $\alpha$  is equal to 1 in the Ohm's law region, is larger than 2 in the trap-filled limit region, and is equal to 2 in the trap-free square law region under a high electric field. As shown in the image, a very good linear relationship is existed.

Results showed that the leakage-current behavior was dominated by the SCLC mechanism, consistent with the leakage mechanism reported in previous literature. However, excluding the SE and PF on the basis of only the above linear fitting was difficult. In other words, the electrical

characteristics may have been consequences of SCLC, SE and PF.

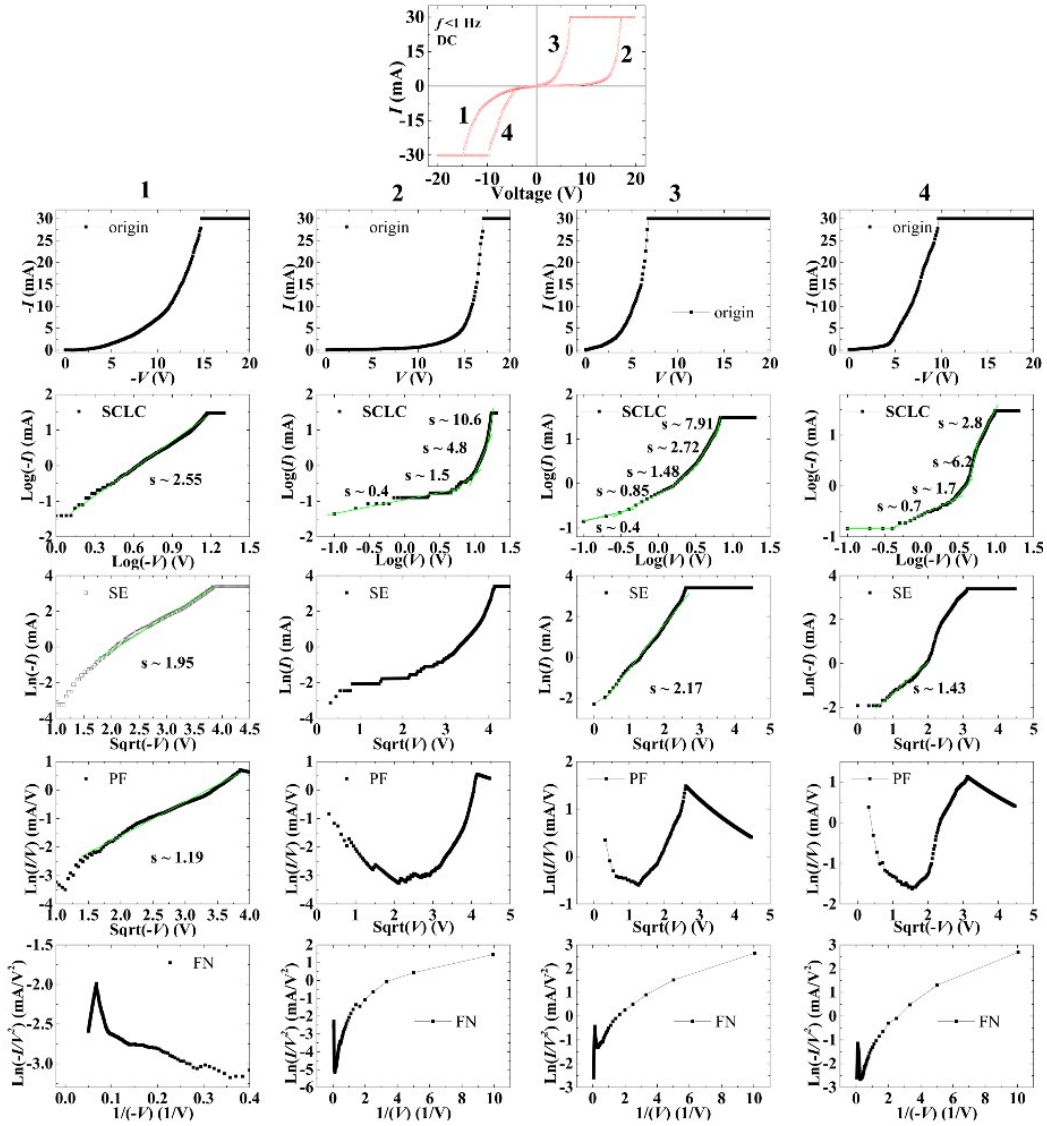


Fig. S4 Plots of the  $I$ - $V$  curves in Fig. 1(e) on different scales to reveal their conduction mechanisms: space-charge-limited conduction (SCLC), Schottky emission (SE), Poole–Frenkel emission (PF) and Fowler–Nordheim (FN) tunneling.

For large-voltage situations, only the SCLC mechanism fitted the data perfectly. It is a body-limited leakage mechanism.

The part with large resistance in the conductive channel plays a decisive role in the total resistance. Therefore, the conduction mechanism is the origin of the resistance in the large-resistance part of the conductive channel. Under the DC small signal, we used various models to fit the current-

voltage data, and found the coexistence of SCLC, SE and PF mechanisms. This shows that the contributions of various mechanisms to the total resistance are not much different. This is different from a single SCLC mechanism under a large DC voltage. Under large voltages, the migration of charged ions causes the restriction of space charge on the movement of carriers.

In summary, a space-charge limiting-current mechanism appeared at low frequencies and large voltages. At DC and low voltages, various electrical-transport mechanisms (SCLC, SE and PF) worked together and were coupled to each other. At high voltages, we attributed the electrical-transport mechanism to the electroforming mechanism of conductive fibers caused by ion migration, consistent with the mechanism of most oxides. To prepare stable ferroresistive devices, we should avoid applying voltage exceeding the voltage required for electroforming.

#### **References:**

1. H. Peng, G. Li, J. Ye, Z. Wei, Z. Zhang, D. Wang, G. Xing and T. Wu, Electrode dependence of resistive switching in Mn-doped ZnO: Filamentary versus interfacial mechanisms, *Appl. Phys. Lett.*, 2010, **96**, 192113.
2. T. Fujii, M. Kawasaki, A. Sawa, Y. Kawazoe, H. Akoh and Y. Tokura, Electrical properties and colossal electroresistance of heteroepitaxial SrRuO<sub>3</sub>/SrTi<sub>1-x</sub>Nb<sub>x</sub>O<sub>3</sub> (0.0002 ≤ x ≤ 0.02) Schottky junctions, *Phys. Rev. B* 2007, **75**, 165101.
3. A. Odagawa, H. Sato, I. Inoue, H. Akoh, M. Kawasaki, Y. Tokura, T. Kanno and H. Adachi, Colossal electroresistance of a Pr<sub>0.7</sub>Ca<sub>0.3</sub>MnO<sub>3</sub> thin film at room temperature, *Phys. Rev. B*, 2004, **70**, 224403.
4. J. G. Simmons, Poole-Frenkel effect and Schottky effect in metal-insulator-metal systems, *Phys. Rev.* 1967, **155**, 657.
5. S. M. Sze, *Physics of Semiconductor Devices*, 2nd ed. (Wiley, New York, 1981). (John Wiley & sons, 1981).
6. M. A. Lampert and P. Mark, *Current Injection in Solids* (Academic, New York, 1970).